



HAL
open science

Rolled knitted scaffolds based on PLA-pluronic copolymers for anterior cruciate ligament reinforcement: A step by step conception

Coline Pinese, Adrien Leroy, Benjamin Nottelet, Christian Gagnieu, Jean Coudane, Xavier Garric

► To cite this version:

Coline Pinese, Adrien Leroy, Benjamin Nottelet, Christian Gagnieu, Jean Coudane, et al.. Rolled knitted scaffolds based on PLA-pluronic copolymers for anterior cruciate ligament reinforcement: A step by step conception. *Journal of Biomedical Materials Research Part B: Applied Biomaterials*, 2017, 105 (4), pp.735-743. 10.1002/jbm.b.33604 . hal-02387436

HAL Id: hal-02387436

<https://hal.umontpellier.fr/hal-02387436>

Submitted on 24 Jan 2024

HAL is a multi-disciplinary open access archive for the deposit and dissemination of scientific research documents, whether they are published or not. The documents may come from teaching and research institutions in France or abroad, or from public or private research centers.

L'archive ouverte pluridisciplinaire **HAL**, est destinée au dépôt et à la diffusion de documents scientifiques de niveau recherche, publiés ou non, émanant des établissements d'enseignement et de recherche français ou étrangers, des laboratoires publics ou privés.

Rolled knitted scaffolds based on PLA-pluronic copolymers for anterior cruciate ligament reinforcement: A step by step conception

Coline Pinese,¹ Adrien Leroy,¹ Benjamin Nottelet,¹ Christian Gagnieu,² Jean Coudane,¹ Xavier Garric¹

¹Department of Artificial Biopolymers, Max Mousseron Institute of Biomolecules (IBMM), UMR CNRS 5247, University of Montpellier, Faculty of Pharmacy, 15 Av. C. Flahault, Montpellier, 34093, France

²National Institute of Applied Science, MATEIS, UMR 5510, Equipe I2B -, INSA de Lyon, Université Claude Bernard Lyon1, Villeurbanne, France

Abstract: The aim of this study was to prepare a new knitted scaffold from PLA-Pluronic block copolymers for anterior cruciate ligament reconstruction. The impact of sterilization methods (beta-ray and gamma-ray sterilization) on copolymers was first evaluated in order to take into account the possible damages due to the sterilization process. Beta-ray radiation did not significantly change mechanical properties in contrast to gamma-ray sterilization. It was shown that ACL cells proliferate onto these copolymers, demonstrating their cytocompatibility. Thirdly, in order to study the influence of shaping on mechanical properties, several shapes were created with copolymers yarns: braids, ropes and linear or rolled

knitted scaffolds. The rolled knitted scaffold presented interesting mechanical characteristics, similar to native anterior cruciate ligament (ACL) with a 67 MPa Young's Modulus and a stress at failure of 22.5 MPa. These findings suggest that this three dimensional rolled knitted scaffold meet the mechanical properties of ligament tissues and could be suitable as a scaffold for ligament reconstruction. © 2016 Wiley Periodicals, Inc. *J Biomed Mater Res Part B: Appl Biomater*, 105B: 735–743, 2017.

Key Words: ligament reinforcement, soft tissues, biomaterials, PLA-pluronic, sterilization

INTRODUCTION

The anterior cruciate ligament (ACL) plays an important role in knee stability and functional movements. Following accidents or vigorous sports activities, ACL injuries frequently occur. In the United States, there are between 100,000 to 200,000 ACL injuries annually.^{1,2} These injuries can be the consequence of a simple rupture of some fibers or a complete rupture of the ligament. ACL injuries can cause short-term (instability) and long-term (osteoarthritic degeneration) complications.

The implantation of autograft tendon tissue is the gold standard surgical technique thanks to its good initial mechanical strength and cell proliferation capacity. However, it was shown that up to 19% of autologous transplants require surgical revision 10 years following surgery.³ Graft failures are caused by several factors like technical errors or a lack of graft maturation. In addition, this therapeutic solution requires a donor site (usually the operated knee, sometimes the contralateral knee), which increases the morbidity and the length of time required for surgery. To overcome this problem, allografts can be used. However, there are many associated disadvantages such as risk of infection,

increased transmitted diseases, reduced graft strength, immune rejection, or delayed incorporation.⁴

Non degradable artificial ligaments, such as Leeds-Keio[®], Proplast[®], Gore-Tex[®], and Stryker-Dacron[®] have also been used in ACL repair, because they overcome drawbacks of biological grafts. Many long-term ruptures or synovitis due to debris were observed, demonstrating that these artificial devices are limited to reinforcement and do not provide a complete tissue integration.⁵

The emergence of degradable materials allows the arrival of new hopes for ligament regeneration. Degradable materials can provide temporary mechanical supports that degrade progressively and are colonized by surrounding tissues until complete substitution by neotissue. Many biomechanical considerations should be taken into account when designing ligament tissue reinforcement. The scaffold should ideally fulfill all requirements of the healthy ACL. The main mechanical features of native ligaments are stiffness, reflected by a Young's modulus of 50–150 MPa and strain at failure of 16–36 MPa for ACL.⁶ PLLA braids have been designed as a total temporary reinforcement.^{7–9} This shape has a particular interest because of its high stress at

failure (81.6 MPa). However, with a Young's modulus of 757 Mpa this scaffold is too rigid and, accordingly, has a low deformability with a 4% toe-region strain value. Moreover, it has been shown that low braid porosity interfere with cell penetration and nutriment distribution¹⁰ in the center of the braid. In consequence, cells surround braid without succeeding in scaffold penetration. Knitted shapes give an opportunity to create elastic template with a better tissue penetration.

Although particularly popular thanks to its degradable properties and good biocompatibility, poly(lactide)s (PLAs) do not present optimal mechanical properties to replace soft tissues like ligaments, tendons, cartilage or blood vessels.^{11,12} In order to obtain a degradable material that may meet specific requirements of the ligament reconstruction in terms of mechanical properties and degradation time, our group synthesized a new family of high molecular weights PLA-Pluronic®-PLA copolymers.¹³ We showed the possibility of modulating both mechanical and degradation properties by changing the crystallinity of PLA blocks and the initial global molecular weight. Degradation rates associated with good cytocompatibility make those PLA-based copolymers appropriate as materials for the conception of scaffolds for ligament reconstruction.

The goal of this work is to develop a scaffold whose composition and design fit with ligament regeneration. We hypothesized that the combination of PLA-Pluronic based copolymers and adequate shapes can allow the conception of a ligament substitute that meets specific requirements of the ligament reconstruction in terms of mechanical properties. We first evaluated the impact of two sterilization methods (beta-ray and gamma-ray sterilization) on copolymers. Then, ACL cell viability and behavior on these copolymers were studied. As good mechanical properties are a key parameter in ligament reinforcement conception, we studied the influence of scaffold shapes on mechanical properties. 2D and 3D shapes have been created in order to design a scaffold with mechanical properties as close as possible to those of native anterior cruciate ligament (ACL).

MATERIALS AND METHODS

Materials

Poloxamer (Pluronic® F-127; 12,600 g mol⁻¹), tin(II)2-ethylhexanoate (Sn(Oct)₂, 95%), dichloromethane (DCM), diethyl ether and tetrahydrofuran (THF) were purchased from Sigma-Aldrich (St-Quentin Fallavier, France). D-Lactide (D-LA), L-lactide (L-LA), and D,L-lactide (D,L-LA) were purchased from Purac (Lyon, France). Dulbecco's Modified Eagle Medium (DMEM) Nut Mix F-12, calf fetal serum, L-glutamine, phosphate-buffered saline (PBS), penicillin, streptomycin, amphotericin B and non-essential amino acid were purchased from Gibco (Saint Aubin, France). 12-well nonadhesive culture plates were purchased from Becton Dickinson (Le Pont de Claix, France) and Viton® O-rings from Radiospares (Beauvais, France). All chemicals and solvents were used without purification.

Copolymers synthesis

We synthesized PLA94-Pluronic®-PLA94 block copolymers with two molecular weights (200 kg mol⁻¹ and 400 kg mol⁻¹; named 94P200 and 94P400) and a 200 kg mol⁻¹ PLA polymer (named 94-200). Polymers were synthesized following a procedure previously described by our group.¹³ Typically, predetermined amounts of lactide and Pluronic® or benzyl alcohol were introduced into a flask and tin(II) 2-ethylhexanoate (0.1 molar % with respect to lactic acid units) was then added. After degassing, the flask was sealed under vacuum and polymerization was allowed to proceed at 110°C. After 5 days, the copolymer was recovered by dissolution in dichloromethane and precipitation in cold diethyl ether. Finally, the product was dried under reduced pressure to constant mass. Copolymers were obtained with an average yield of 88%.

Sterilization

To evaluate the impact of sterilization on 94P200 copolymers, sample plates were prepared by compression of 3 g of copolymer under 8 tons using a Carver press in stainless steel mould for 10 min at 200°C. A first group of 4 samples was sterilized under normal atmosphere by gamma-ray, between 31.5 and 39 kGy, whereas a second group of 4 samples was sterilized by beta-ray between 25 and 27 kGy by the company Ionisos, France.

Characterization

Number average molecular weight (M_n) and dispersity (D) of polymers were determined by size exclusion chromatography (SEC) using a Viscotek GPCMax autosampler system fitted with two Viscotek LT5000L Mixed Medium columns (300 × 7.8 mm). Polymer solution (10 mg mL⁻¹ in tetrahydrofuran) was filtered through a 0.45 μm Millipore filter before injection of 20 μL of filtered solution. M_n was expressed according to calibration using Polystyrene standards.

Differential scanning calorimetry (DSC) measurements were carried out under nitrogen on a Perkin Elmer Instrument DSC 6000 Thermal Analyzer. Samples ($n = 4$) were submitted to a first heating scan to 200°C (10°C min⁻¹), followed by a cooling scan from 200°C to -30°C (7°C min⁻¹) and a second heating scan to 200°C (10°C min⁻¹). Glass transition temperature (T_g) or relaxation (T_r), cold recrystallization temperature (T_{cc}), melting temperature (T_m), and melting enthalpy (ΔH_m) were measured on the second heating ramp for sterilization impact, to erase shaping influence. The first heating ramp was used to study yarn thermal properties.

Proliferation studies

Primary ligamentocytes, extracted from rat's ACL, were cultured in DMEM Nut Mix F-12 supplemented with 10% of decomplexed calf fetal serum, 4 mM of L-glutamine, 1.5 g L⁻¹ of NaHCO₂, 5000 U.mL⁻¹ penicillin, 5000 mg mL⁻¹ streptomycin, 2.5 μg mL⁻¹ of amphotericin B, and 1% (v/v % in DMEM/F12) of non-essential amino acid.

Ligaments were obtained from another *in vivo* study that includes the taking of ligament. All animals were treated according to institutional guidelines of laboratory and animal treatment and care. All experiments were approved by the animal research committee.

Sample disks were cut (3.9 cm²) from 94P400 and 94P200 copolymer films and were sterilized with beta-ray. Disks were placed in TCPS 12-well non adhesive culture plate. Sinkers were used to maintain them at the bottom of wells. Second-passage rat ligamentocytes were used and seeded at 25,000 cells per well in triplicate. After 2 h of adhesion, the culture medium was added to immerse all samples. The same seed was performed in cell culture treated wells (control). Disks were incubated at 37°C and 5% CO₂. Cell quantification was performed by measurement of viability with MTT (3-(4,5-dimethylthiazol-2-yl)-2,5-diphenyltetrazolium bromide) after 2, 6, and 12 days of culture. Typically, the medium was aspirated, samples were rinsed with PBS and 1.5 mL of PBS solution containing 0.5 mg mL⁻¹ of MTT was added. After three hours (± 15 min) of incubation, formazan blue was dissolved in 1 mL of DMSO and after 40 min of shaking, absorbance was measured at 600 nm.

Copolymers scaffold conception

Yarn conception. Spinning was carried out with a pilot spinning machine (Centexbel, Gent, Belgium). Copolymers 94P200, 94P400, and polymer 94-200 under the form of small pellets were placed in a dryer for 2 days to remove any residual moisture. Copolymers were heated at 200°C during 10 minutes and then pressurized to cross a 1.5 mm diameter die with a 10 rpm spinning speed. Obtained monofilaments passed through an air flow to be cooled and were carried to a drawing frame composed of six 50°C rolls. The rolls rotational speed of 20 rpm and 40 rpm define a draw ratio (DR) of 2 and 4 for monofilaments. Mean diameter corresponds to the mean of 10 measurements of monofilament taken on different part of filaments.

Textile conception. In order to study the mechanical properties of 94P400 yarns, we produced different shapes: linear knitted textiles, hollow knitted ropes, braids and rolled knitted scaffolds. For linear knitted textiles and hollow knitted ropes conception, monofilaments were first coated by batching silicon oil in order to be protected from important friction forces in the knitted process. Three monofilaments were then twisted to create a multifilament yarn. This multifilament yarn was knitted with a Silver Reed SK270 knitted machine to obtain linear knitted fabrics (2 cm of width) and hollow ropes (with a diameter of 8 mm). Silicon batching oil has been removed by 3 \times 15 min baths of sodium lauryl sulfate (v/v 1%) in ultrasound bath. For braids conception, three bundles of ten monofilaments were braided by hand to produce a 3.5 mm width braid. Rolled knitted scaffolds were made using the linear knitted shape. Linear knitted fabrics were rolled twice on themselves to form a 1-cm-diameter tube. The fabric edges were sewn to maintain tubular fabrics shapes.

Mechanical properties studies

For mechanical properties studies, beta-ray sterilized plates obtained by hot molding (30 \times 10 \times 0.5 mm), beta-ray sterilized yarns and beta-ray sterilized textiles were analyzed with an Instron 4444 at a crosshead speed rate of 5 mm min⁻¹, each sample being loaded to failure. 2 cm \times 3 cm of linear knitted fabrics, 3 cm of hollow ropes (diameter of 8 mm), 3 cm of a 3.5 mm width braid and 3 cm of rolled knitted scaffold (1-cm-diameter tube) were analyzed. Each sample was analyzed at 37°C in triplicate and Young's modulus (E , MPa), stress at failure (δ_b , MPa), strain at failure (ϵ_b , %), yield stress (δ_y , MPa), and yield strain (ϵ_y , %) were expressed as the mean value of the three measurements. Young's Modulus was calculated using the initial linear portion of the stress/strain curve.

In order to study the behavior under cyclic loads, 50 cyclic deformations were imposed on 3 rolled knitted scaffold. Tensile load was recorded using a sinusoidal strain profile according to the following regimens: 0% strain amplitude (subphysiologic) to 10% strain amplitude (supra-physiologic) which corresponds to the pathological elongation. Commercial polyethylene terephthalate (PET) ligament reinforcement from Orthomed was used as reference.

Statistical analyses

Results corresponded to separate experiments done in triplicate and values are given as mean \pm standard deviation (SD). Statistical analyses were performed with the SigmaStat software. Comparison between several groups used a non-parametric Kruskal-Wallis (a level of $p < 0.05$ was considered statistically significant). To study cells proliferation, comparison of material values for each times have been done with a Wilcoxon signed rank test (a level of $p < 0.05$ was considered statistically significant).

RESULTS

Sterilization study

The first part of the sterilization study was to select the sterilization method that impacts as little as possible the properties of copolymers. For this purpose, the influence of gamma and beta-ray sterilization processes on the molecular weight, the thermal and mechanical properties of the 94P200 copolymer were evaluated.

As shown in Table I, copolymer molecular weights were halved after sterilization process, from 114 kg mol⁻¹ in unsterilized copolymer to 52 kg mol⁻¹ and 45 kg mol⁻¹ in beta-ray and gamma-ray sterilized copolymers, respectively. Dispersity of polymers after sterilization is relatively close to initial dispersity. The copolymer molecular weight loss has consequences on mechanical properties. Gamma-ray sterilized copolymers have a higher Young's modulus (867 \pm 27 Mpa) and a lower strain at failure (10.3 \pm 1.86%) than unsterilized material with values of 555 \pm 50 MPa and 613 \pm 37%, respectively. The low strain at failure value illustrates the brittleness of 94P200 after gamma radiation sterilization.

In contrast, beta-ray sterilized materials show no significant different Young's modulus and strain at failure, with

TABLE I. Molecular Weight (M_n), Mechanical, and Thermal Properties of Unsterilized (Control), Gamma and Beta-Ray Sterilized 94P200 Copolymer: Polymers Dispersity (\mathcal{D}), Young Modulus (E), Stress at Failure (σ_f), Strain at Failure (ϵ_f), Melting Temperature (T_m), Melting Enthalpy (ΔH_m), Glass Transition Temperature (T_g) Are Reported

Sterilization	M_n (g mol ⁻¹)	\mathcal{D}	E (MPa)	σ_f (MPa)	ϵ_f (%)	T_m (°C)	ΔH_m (J/g)	T_g (°C)
Control	114 000	1.59	555 ± 50	18.0 ± 1.6	613 ± 37	148	10.06	46.3
Gamma ray	45 000	1.85	867 ± 27	15.4 ± 5.8	10.3 ± 1.86	149	13.12	49.3
Beta ray	52 000	1.70	452 ± 100	13.0 ± 2.0	544 ± 25	148	28.0	43.2

value of 452 ± 100 MPa and $544 \pm 25\%$, respectively ($p = 1$ and $p = 0.1$, respectively). Despite the molecular weight loss induced by beta-ray sterilization, we observed that copolymer mechanical properties were only slightly modified. Melting enthalpy values of beta-ray sterilized copolymers (28.0 J g^{-1}) are higher than values observed for gamma-ray sterilized (13.12 J g^{-1}) and unsterilized copolymers (10.06 J g^{-1}). Furthermore the glass transition temperature of beta-ray sterilized copolymer (43.2°C) is lower than those obtained for gamma-ray sterilized (49.3°C) and unsterilized copolymers (46.3°C).

Cell proliferation

Tissues regeneration template should allow cell proliferation. In order to study cells behavior on two different sterilized copolymers, proliferation of ACL rat's ligamentocytes on copolymers films or in TCPS wells (control) was compared using the MTT assay during a 12-day period. As shown in Figure 1, ACL rat's ligamentocytes highly proliferated during the overall period for all copolymers. Even if the proliferation rate of the control is higher than those obtained for both copolymers, the absorbance values significantly increased during a period of 12 days ($p < 0.001$) and no difference between the two copolymers was observed. These results suggest that sterilized copolymers are compatible with primary rat ligamentocytes cell proliferation.

Yarn and textile conception

Yarns characterization. Microfilaments or yarns have been made from 94-200 polymer, 94P200, and 94P400 copolymers. Table II presents mechanical and thermal characteristics of 94-200 polymer, 94P200, and 94P400 copolymers. Mechanical properties of yarns without stretching (draw ratio, DR = 0) could not be analyzed because of the weak copolymer chain cohesion. Yarn diameter varies with DR. Indeed, 94P200 yarns have a $1099 \mu\text{m}$ diameter without stretching (DR = 0), a $392 \mu\text{m}$ diameter and a $188 \mu\text{m}$ diameter with DR of 2 and 4, respectively. Table II shows that the DR has also several consequences on thermal properties. First, the melting enthalpy (ΔH_m) increases with DR from 9.03 J g^{-1} for 94P200 yarns without stretching to 19.6 J g^{-1} and 21.58 J g^{-1} for DR of 2 and 4, respectively. It shows that there is an increase of copolymers chains alignment and therefore of copolymer crystallinity with the DR expand. The increase of relaxation peak temperature from a DR value of 4 confirms this observation. 94P200 yarns relaxation occurs at 49.9°C without stretching and at 50.7°C

and 56.8°C for DR of 2 and 4, respectively, suggesting that more energy is necessary to obtain mobility between copolymer chains. The decrease of cold crystallization temperature (T_{cc}) and the increase of related enthalpy (ΔH_c) show that the crystallization process is faster and more important for the stretched yarns. For 94P200 yarns, it takes place at 116°C without stretching ($\Delta H_c = -8.4 \text{ J g}^{-1}$) and 74.2°C for a stretched yarn with a DR of 4 ($\Delta H_c = -17.79 \text{ J g}^{-1}$). This requires less energy to rearrange copolymers chains. Same consequences of DR are visible on 94P400 and 94-200.

Tensile tests show that mechanical properties of 94P200 yarns are influenced by the DR (Table II). 94P200 yarns with a DR of 4 have a higher Young's modulus (1311 ± 103 MPa) and stress at failure (84.8 ± 14.2 MPa) compared to the same material with a DR of 2 ($E = 438.56 \pm 56$ MPa and $\sigma_r = 20.9 \pm 3.7$). Chains alignment induced by stretching increases copolymers crystallinity and therefore the stiffness. Accordingly, copolymers yarns become less deformable with a strain at break of $638 \pm 127\%$ for yarns with a DR of 2 and of $224 \pm 104\%$ for yarns with a DR of 4. Same consequences of DR are visible on 94P400 and 94-200.

Yarns have an interesting mechanical strength, compatible with ALC mechanical properties, even more when the copolymer molecular weight is high. 94P200 yarns present a stress at failure of 84.8 ± 14.2 MPa which is lower than 94P400 yarns with a value of 132 ± 38 MPa. Yarns composed of 400 kg mol^{-1} copolymers present a high strength. Accordingly, their stiffness is higher and their strain at break lower. Moreover, the influence of copolymerization is visible on mechanical properties. The block structure is

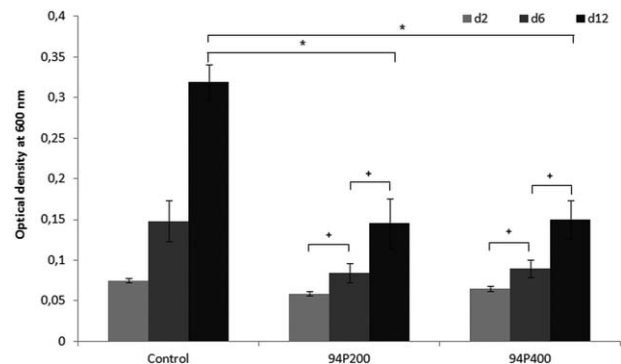


FIGURE 1. Anterior cruciate ligament cells proliferation after 12 days on TCPS (control), beta-ray sterilized 94P200 and beta-ray sterilized 94P400 copolymers films (d = days). Data are means \pm SD, $n = 3$. Kruskal-Wallis test compared to control, $*p < 0.05$ and Wilcoxon test to compare times $+p < 0.05$.

TABLE II. Mean Diameter, Mechanical, and Thermal Properties of Beta-Ray Sterilized Polymer Yarns: Melting Temperature (T_m), Melting Enthalpy (ΔH_m), Relaxation Temperature (T_r), Cold Recrystallization Temperature (T_{cc}), Recrystallization Enthalpy (ΔH_c), and Young Modulus (E), Stress at Failure (σ_f), Strain at Failure (ϵ_f) Are Reported

Polymers	DR	Mean diameter (μm)	T_m ($^{\circ}\text{C}$)	ΔH_m (J/g)	T_r ($^{\circ}\text{C}$)	T_{cc} ($^{\circ}\text{C}$)	ΔH_c (J/g)	E (Mpa)	σ_f (Mpa)	ϵ_f (%)
94P200	0	1099 ± 47	149.64	9.03	49.99	116	-8.39	—	—	—
94P200	2	392 ± 36	149.99	19.6	50.69	102.71	-8.67	438 ± 56	20.9 ± 3.7	638 ± 127
94P200	4	188 ± 7	150.16	21.58	56.85	74.21	-17.79	1311 ± 103	84.8 ± 14.2	224 ± 104
94P400	0	1569 ± 38	149.26	2.9	55.77	121.95	-2.49	—	—	—
94P400	4	118 ± 9	150.13	25.71	59.5	84.84	-3.89	2514 ± 20	132 ± 38	183 ± 10
94-200	0	1111 ± 57	149.01	1.78	60.51	126.01	-1.39	—	—	—
94-200	4	131 ± 26	148.82	10.11	64.17	124.36	-7.49	1591 ± 158	54.9 ± 4.72	60.5 ± 34.9

responsible for an important increase of strain at failure. Indeed, 94P200 breaks at a strain of $224 \pm 104\%$ and 94-200 breaks at a strain of $60.5 \pm 34.9\%$.

Textile characterization. The 94P400 yarns have been chosen to produce several fabrics because of their interesting mechanical properties. Multifilament linear knitted textile,

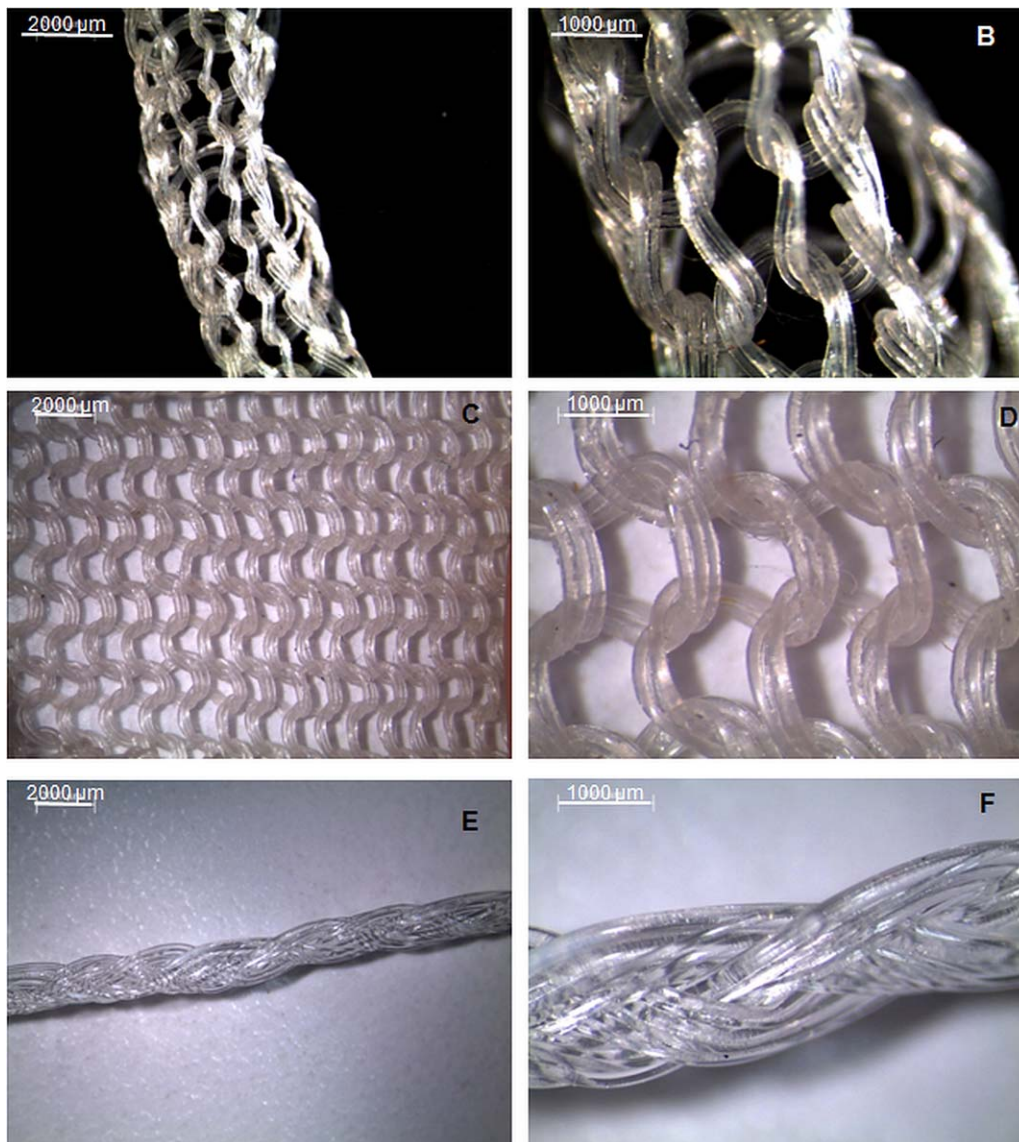
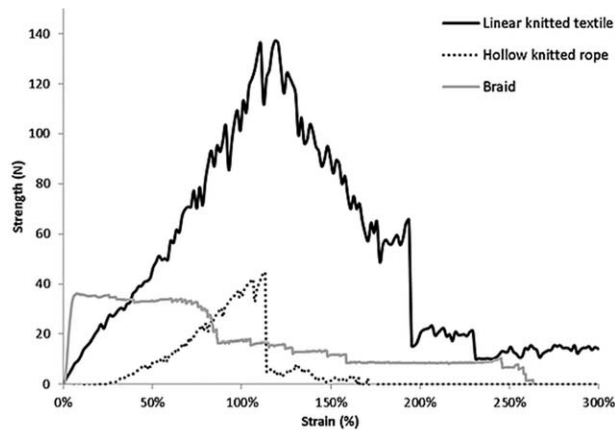


FIGURE 2. 94P400 multifilament hollow knitted rope, 94P400 multifilament linear knitted textile, and 94P400 braid.



Shape	Stiffness (N.mm ⁻¹)	Strength at failure (N)
Linear knitted textile	98.3	140
Braid	463.7	33
Hollow knitted rope	86	57

FIGURE 3. Typical strength and stress curves of scaffold with different shapes and associated stiffness and strength at failure values.

multifilament hollow knitted rope and braid were designed (Figure 2). Mechanical properties of the fabrics were evaluated in order to identify the more suitable for ligament reconstruction. Figure 3 shows stress–strain curves for the different shapes. It can be first observed that stiffness varies according to the textile shape. Indeed, the braid has a higher stiffness value (463.7 N mm⁻¹) compared to linear knitted textile (98.3 N mm⁻¹) and hollow knitted rope (86 N mm⁻¹). In comparison, ACL stiffness is between 100 and 400 N mm⁻¹ ⁶ and therefore braids seems to be too rigid. Braid and hollow knitted rope are also less resistant than linear knitted textile with strength at failure of 33N, 57N, and 140N, respectively. Moreover, the deformation profile under solicitation is different between knitted shapes and braid: the irreversible deformation occurs earlier for braid shape (7.5%).

As resistance is one of the key parameters of mechanical properties, we decided to improve linear knitted textile with the creation of a rolled knitted scaffold. The conception of a 3D shape is also interesting to mimic ligament tissue conformation. The mechanical properties of rolled knitted scaffold are presented in Figure 4(A,B). The strain and stress profile is similar to ligaments, with a toe-region (I), which is the progressive fibers recruitment, a linear region (II), corresponding to the fibers switched on and a breaking zone (III). As collagen of ACL, knitted degradable fibers will gradually be recruited and arranged in the stress direction, giving a 67 MPa Young's modulus. Rolled knitted scaffold can be reversibly deformed to 27.2% of its initial deformation. It is broken for a 90% deformation of its original length and for a stress at failure of 22.5 MPa. As a comparison, ACL has a Young's modulus between 50 and 150 MPa, a toe-region limited to 2–5% and a stress at failure between

16 and 36 Mpa.⁶ Rolled knitted scaffold has a similar strain and stress profile and mechanical characteristic values are close to those of ACL.

In order to play a role as ligament reinforcement, rolled knitted scaffold must be able to undergo loading cycles. Figure 4(B) illustrates rolled knitted scaffold behavior under cyclic solicitations. The cycle of the first charge is slightly different due to the material accommodation of the load. Thereafter, responses to other cyclic solicitations are similar. After each cycle, rolled knitted scaffold returns to its initial state and the necessary force to deform the scaffold is the same after 2 or 50 cycles. Furthermore, the shape of the cycle shows that during the cycle, the rolled knitted scaffold is still in a reversible deformation phase. The rolled knitted scaffold is elastic in physiological deformation zone (between 0 and 8%)⁶ allowing knee movements without being damaged.

A comparison with a commercial PET for total reinforcement and the copolymer rolled knitted scaffold is shown in Figure 5. The main advantage of PET commercial total reinforcement is the stress at failure of 51.27 MPa which is higher than ligaments and its strain at failure that is above the values corresponding to the physiological zone. However, the commercial PET for total reinforcement shows an important stiffness as compared to ligaments, with a Young modulus of 877 MPa and a low deformation capacity with a yield strain of 3.75%. The irreversible deformation phase is

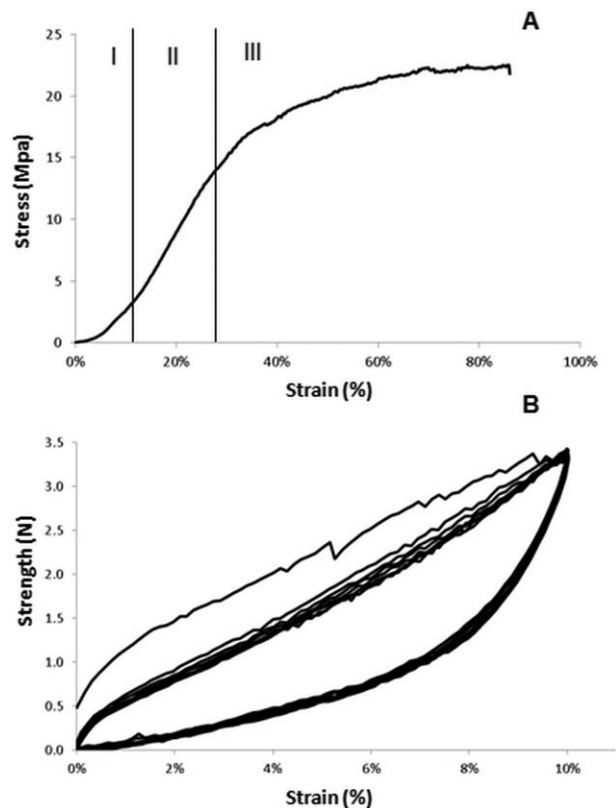
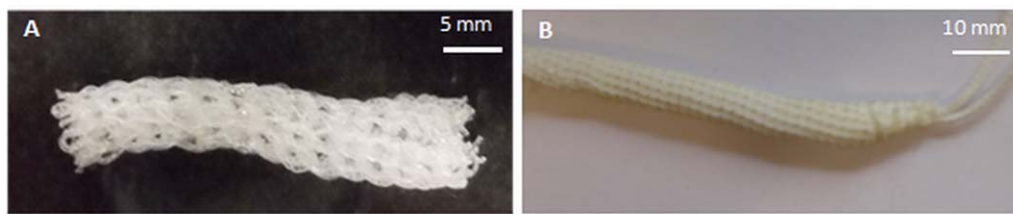


FIGURE 4. Rolled knitted scaffold strain and stress curve, and strain and strength curve of rolled knitted fabric under cyclic loads.



Mechanicals properties	ACL Ligaments ⁶	Rolled knitted scaffold	PET commercial reinforcement
Young Modulus (MPa)	50-150 Mpa	67 MPa	877 MPa
Yield strain (%)	7-16 %	27.20%	3.75%
Stress at failure (MPa)	16-36 Mpa	22.5 Mpa	51.27 MPa
Strain at failure (%)	19-36 %	90%	17%

FIGURE 5. Illustrations of rolled knitted scaffold and PET commercial total reinforcement, mechanical characteristics of native ligament, rolled knitted fabric, and PET commercial reinforcement (Orthomed).

reached in the physiological deformation zone which will strongly impact the reinforcement mechanical behavior.

The knitting process involves silicone oil to lubricate the yarn and, as silicon oil can hamper the cell compatibility, we developed a method to remove oil silicon. A surface analysis by Infra-Red Spectroscopy was used to confirm the disappearance of specific peaks corresponding to silicon oil (data not shown). Then, the cytocompatibility of the final knitted structure after silicon oil removing was tested. Cytocompatibility of rolled knitted scaffold after removing silicon oil was assessed by measuring ligamentocyte viability by using MTT test after 24 h on the scaffold and on TCPS control (Supplementary Data 1). The OD values corresponding to living cells on rolled knitted scaffold are very close to OD values of TCPS control suggesting that the scaffold after silicon oil removing step is cytocompatible.

DISCUSSION

A resorbable fabric for ACL reconstruction should provide a load-bearing framework that present suitable strength and cell compatibility to promote ligament formation for long-term. The main objective of this work was to determine the optimal shape for scaffolds based on PLA-Pluronic block copolymers for anterior cruciate ligament reconstruction.

Sterility is a mandatory step to ensure absence of viable microorganisms responsible of harmful reaction *in vivo*. Linear block copolymers PLA-Pluronic-PLA (200 kg mol⁻¹ named 94P200) were synthesized and consequences of two sterilization methods on their mechanical and thermal properties were studied. We showed that gamma and beta-ray sterilization induced chain random cuts resulting in a significant loss of molecular weight. Several studies have shown that, on PLA materials, gamma radiation is responsible for a molecular weight loss of 50% by chain scission.^{14,15} Chains arrangements after gamma sterilization strongly modify the 94P200 copolymer mechanical properties, which is not the

case of beta-ray sterilization. Two phenomena can explain this difference: a partial crosslinking or an increase of crystallinity by chain scission. Molecular weight loss and tensile strength values suggest that chain scissions are predominant. With higher values of melting enthalpy, beta-ray sterilized 94P200 copolymers are more crystalline than gamma ray sterilized or unsterilized copolymers. This may be an explanation for the slight modification of beta-ray sterilized copolymers mechanical properties. The weaker impact of beta ray-sterilization as compared to gamma ray-sterilization was also reported on PLA microspheres.¹⁶ In order to improve it, we decided to synthesize higher molecular weight copolymers (400 kg mol⁻¹ named 94P400). Yarns have been made from PLA94 homopolymer (200 kg mol⁻¹ named 94-200) and PLA-Pluronic-PLA copolymers (200 kg mol⁻¹ named 94P200 and 400 kg mol⁻¹ named 94P400). We show that ALC ligamentocytes proliferate on both sterilized 94P200 and 94P400 copolymers during at least 12 days.

Initially, yarns were made by melt spinning and mechanical properties were optimized through a step of yarn stretching. This stretching step was used to decrease yarns diameter to facilitate the knitting process and concomitantly copolymer crystallinity was increased. This change affected yarns mechanical properties making them less deformable, but also more resistant. Mechanical properties comparison between 94-200 and 94P200 yarns shows the interest of copolymerization. Indeed, 94P200 and 94-200 present a Young modulus of 1311 ± 103 MPa and 1591 ± 158 MPa, respectively and a strain of 224 ± 104% and 60.5 ± 34.9%, respectively. Blocks introduction might interfere with polymer chains organization which is probably responsible of a strain at failure and a stiffness decreases. This property may be interesting for polymers used for the conception of fabrics that undergo cyclic solicitations. Moreover, yarns resistance will increase with higher DR and molecular

weight. Given that 94P400 yarns with a DR of 4 have an interesting stress at failure, this copolymer has been chosen to process the shaping.

Several shapes were compared to identify the best scaffold able to meet the ligament mechanicals properties requirement. In comparison with a braided structure, knitted textiles offer a lower stiffness, an interesting deformation profile and strength at failure. This is consistent with our previous work on braided twisted shape.¹⁷ Indeed, the irreversible deformation of braided twisted shape occurs for low deformations which is not compatible with a tissue that has to meet important cyclic loads of knees. Furthermore, the scaffolds loss of mechanical properties due to sterilization is high and could not provide braided twisted scaffold enough properties to meet knee physiological solicitations. In consequence we focus on knitted textile. This shape allows the creation of 2D patches which can be used for other applications like Achilles' tendon or rotator cuff tendon reconstruction. The linear knitted textile also allows the creation of 3D shapes for designing tubular total ligament reinforcements. With a Young's modulus of 67 MPa, an elastic deformation of 27.2% and a tensile strength of 22.5 MPa, characteristic values of rolled knitted scaffold are similar to those of native anterior cruciate ligament.⁶ In cyclic loading, the rolled knitted scaffold backs perfectly its original state after deformation, allowing it to meet knee physiological demands without being damaged.

In the literature, ligament reinforcements based on knitted PLA, PLAGA or silk are found, which are easier to produce through the use of commercial yarns. It is usually difficult to compare data from the literature not only because of the diversity of materials, but also because of the multitude of different units used to express the results. However, Vaquette^{18,19} describes a PLAGA knitted structure coated with poly (L-lactic-co-ε-caprolactone) which present excellent results. Mechanical properties were interesting with a Young Modulus of 150 ± 14 MPa, a stress at failure of 39 ± 2 MPa and a strain at failure of $42 \pm 3\%$. Cells proliferated on the composite scaffolds and synthesized an extracellular matrix which form a fibrous network after 14 days. Ouyang²⁰ described a knitted rolled PLA reinforcement. This scaffold is knitted with a 60 yarns multifilament of 25 μm diameter. As PLA yarns are "ready to use", molecular weight and percentage of L-lactide are not described. Knitted PLA fabrics have a stiffness of 28.4 ± 1.8 N mm⁻¹ and a load at failure of 51.4 ± 3.2 N which is lower than our PLA-Pluronic based copolymer fabric (137N). We compare the rolled knitted scaffold with a Orthomed PET reinforcement. Main advantages of commercial PET total reinforcement are a high stress at failure (51.27 MPa) and a strain at failure out of the physiological zone. However, commercial PET total reinforcement shows an important stiffness and a low yield at failure. The stiffness can impede tissue regeneration and a low yield at failure can strongly impact the reinforcement of elastic mechanical properties in cyclic solicitations. Main mechanical characteristic values of rolled knitted scaffold are in the ligaments range of values. Moreover, an interesting property of those materials is the

degradation ability. Indeed mechanical properties will progressively decrease and material will progressively be replaced by a new ligament. A compromise between degradation time and mechanical properties will be determined and presented in another work. This reinforcement can be a good alternative in tissues engineering.

In terms of limitations, mechanical tests should be performed in conditions that mimic physiological conditions. For example, a daily duration of 2 h of traction–torsion cyclic simultaneous solicitations (10% uniaxial strain and 90° of torsion cycles at 1 Hz) could be more relevant. Another limitation concerns the design of the scaffold and more specifically the extremities. Indeed, the design of the extremities of a ligament substitute is a key point to facilitate the fixation by surgeons and to provide a total ligament reinforcement that could resist perfectly to cyclic solicitation.

CONCLUSION

The goal of this study was to develop a scaffold whose composition and design fit to ligament regeneration. We hypothesized that the combination of PLA-Pluronic based copolymers and adequate shapes can allow the conception of a ligament substitute that meet specific requirements of the ligament reconstruction in terms of mechanical properties. We showed that beta-ray sterilized materials keep better mechanical properties compared to gamma-ray sterilized materials. Copolymers were processed into several fabrics shapes which were mechanically tested. We also report that our knitted textiles show interesting stress at failure and elasticity capacities. Rolled knitted textile shapes present mechanical properties close to those of native ACL ligament tissue. As strength and elasticity are two important mechanical properties in ACL tissues, rolled knitted textile shapes are compatible with ACL ligament tissue replacement. Those mechanical properties and the cell proliferation capability make the knitted copolymers interesting as scaffolds for ligament tissue engineering. In a future work, *in vivo* studies will be performed to evaluate the *in vivo* degradation and the tissue integration of a rolled knitted fabric based on PLA-Pluronic copolymers.

REFERENCES

1. Kim HS, Seon JK, Jo AR. Current trends in anterior cruciate ligament reconstruction. *Knee Surg Relat Res* 2013;25:165–173.
2. Buoncristiani AM, Tjoumakaris FP, Starman JS, Ferretti M, Fu FH. Anatomic double-bundle anterior cruciate ligament reconstruction. *Arthroscopy* 2006;22:1000–1006.
3. Weiler A, Schmeling A, Stohr I, Kaab MJ, Wagner M. Primary versus single-stage revision anterior cruciate ligament reconstruction using autologous hamstring tendon grafts—A prospective matched-group analysis. *Am J Sports Med* 2007;35:1643–1652.
4. Leong NL, Petrigliano FA, McAllister DR. Current tissue engineering strategies in anterior cruciate ligament reconstruction. *J Biomed Mater Res A* 2014;102:1614–1624.
5. De smedt M. Les prothèses du ligament croisé antérieur: Analyse d'un échec. *Acta Med belgica* 1998;64:4.
6. Vieira AC, Guedes RM, Marques AT. Development of ligament tissue biodegradable devices: A review. *J Biomech* 2009;42:2421–2430.
7. Laurencin CT, Freeman JW. Ligament tissue engineering: An evolutionary materials science approach. *Biomaterials* 2005;26:7530–7536.

8. Kwansa AL, Empson YM, Ekwueme EC, Walters VI, Freeman JW, Laurencin CT. Novel matrix based anterior cruciate ligament (ACL) regeneration. *Soft Matter* 2010;6:5016–5025.
9. Freeman JW, Woods MD, Laurencin CT. Tissue engineering of the anterior cruciate ligament using a braid-twist scaffold design. *J Biomech* 2007;40:2029–2036.
10. Guidoin M-F, Marois Y, Bejui J, Poddevin N, King MW, Guidoin R. Analysis of retrieved polymer fiber based replacements for the ACL. *Biomaterials* 2000;21:2461–2474.
11. Surrao DC, Waldman SD, Amsden BG. Biomimetic poly(lactide) based fibrous scaffolds for ligament tissue engineering. *Acta Biomater* 2012;8:3997–4006.
12. Chen B-K, Shen C-H, Chen S-C, Chen AF. Ductile PLA modified with methacryloyloxyalkyl isocyanate improves mechanical properties. *Polymer* 2010;51:4667–4672.
13. Leroy A, Pinese C, Bony C, Garric X, Noël D, Nottelet B, Coudane J. Investigation on the properties of linear PLA-poloxamer and star PLA-poloxamine copolymers for temporary biomedical applications. *Mater Sci Eng C Mater Biol Appl* 2013;33:4133–4139.
14. Nugroho P, Mitomo H, Yoshii F, Kume T. Degradation of poly(L-lactic acid) by gamma-irradiation. *Polym Degrad Stab* 2001;72:337–343.
15. de Tayrac R, Chentouf S, Garreau H, Braud C, Guiraud I, Boudeville P, Vert M. In vitro degradation and in vivo biocompatibility of poly(lactic acid) mesh for soft tissue reinforcement in vaginal surgery. *J Biomed Mater Res B Appl Biomater* 2008;85:529–536.
16. Montanari L, Cilurzo F, Selmin F, Conti B, Genta I, Poletti G, Orsini F, Valvo L. Poly(lactide-co-glycolide) microspheres containing bupivacaine: Comparison between gamma and beta irradiation effects. *J Control Release* 2003;90:281–290.
17. Leroy A, Nottelet B, Bony C, Pinese C, Charlot B, Garric X, Noel D, Coudane J. PLA-poloxamer/poloxamine copolymers for ligament tissue engineering: sound macromolecular design for degradable scaffolds and MSC differentiation. *Biomater Sci* 2015;3:617–626.
18. Vaquette C, Kahn C, Frochot C, Nouvel C, Six JL, De Isla N, Luo LH, Cooper-White J, Rahouadj R, Wang XO. Aligned poly(L-lactico-e-caprolactone) electrospun microfibers and knitted structure: A novel composite scaffold for ligament tissue engineering. *J Biomed Mater Res Part A* 2010;94:1270–1282.
19. Vaquette C, Slimani S, Kahn CJF, Tran N, Rahouadj R, Wang X. A poly(lactic-co-glycolic acid) knitted scaffold for tendon tissue engineering: An in vitro and in vivo study. *J Biomater Sci Polym Ed* 2010;21:1737–1760.
20. Ouyang HW, Toh SL, Goh J, Tay TE, Moe K. Assembly of bone marrow stromal cell sheets with knitted poly (L-lactide) scaffold for engineering ligament analogs. *J Biomed Mater Res Part B* 2005;75:264–271.